



Effects of Thermophoresis, Dufour, Hall and Radiation on an Unsteady MHD Flow past an Inclined Plate with Viscous Dissipation, Chemical Reaction and Heat Absorption and Generation

N. Pandya¹ and A. K. Shukla^{1†}

¹ *Department of Mathematics and Astronomy, Lucknow University, Lucknow-226007, India*

† *Corresponding Author Email: ashishshukla1987@gmail.com*

(Received June 23, 2014; accepted October 15, 2014)

ABSTRACT

This paper investigates study of MHD(Magneto hydrodynamics) flow of viscous incompressible fluid past an inclined porous plate embedded in porous medium with the effects of Thermophoresis, Dufour, Hall, radiation, viscous dissipation, chemical reaction and heat generation or absorption. Non dimensional partial differential equations of governing equations of flow are solved numerically by applying Crank-Nicolson finite difference method for different values of parameters. Velocity, temperature, concentration profiles are discussed through graphs for different values of parameters and skin friction coefficients, Nusselt number and Sherwood number are discussed through tables.

Keywords: MHD, Dufour effect, Thermophoresis effect, Hall effect, radiation effect, Heat and Mass transfer, chemical reaction, Crank-Nicolson method.

1. INTRODUCTION

Large number of mathematicians have been attracted from last many decades toward investigation of unsteady MHD flow with effects of Thermophoresis, Dufour, radiation, chemical reaction, Hall parameter because there are number of avenues for research work. This investigation of such flow has application in MHD generators, soil sciences, nuclear power reactors, aeronautics, chemical engineering and so on.

Thermophoresis, Dufour effects and chemical reaction are significant if density difference exists and reaction level is not low respectively. If an electric field is applied at right angles to magnetic field, the whole current will not flow along the electric field, this nature of the electric current of flow across an electric field in presence of a magnetic field is called Hall effect.

Lee(Lee 2001) has analyzed a combined numerical and theoretical investigation of laminar natural convection heat and mass transfer in open vertical plates with unheated entry and unheated exist for various thermal and concentration boundary conditions. Sudha Karraiah et al.(Karraiah, Kesaraiah, and Bhavana 2013) studied Soret effect on unsteady MHD flow past a vertical plate with heat

source. Postelnicu(Postelnicu 2004) studied numerically the influence of magnetic field on heat and mass transfer by natural convection from vertical surfaces in porous media with Soret and Dufour effects.

Sparrow et al.(Sparrow, Eichhorn, and Gregg 1959) has studied the combined effect of a steady free and forced convection laminar flow and heat transfer between two vertical parallel walls. Alam and Rahman(Alam and Rahman 2006) studied Soret-Dufour effects on unsteady MHD flow in porous medium. Olanrewaju(Oladapo 2010) analyzed Soret-Dufour effects of a transient free convective flow with radiative heat transfer past flat plate moving through a binary mixture and Dufour effects using both linear and non linear stability analysis.

Vempati et al.(Vempati and Gari 2010) has analyzed numerically Soret-Dufour effects on an unsteady MHD flow past an vertical porous plate with thermal radiation. Pandya and Shukla(Pandya and Shukla 2013) studied Soret-Dufour effects on unsteady MHD flow past an inclined porous plate embedded in porous medium. Ghosh(Ghosh 2002) investigated Hall effects on MHD flow in rotating system.

The objective of this work is to study combined effects of Thermophoresis, Dufour, Hall, radiation,

chemical reaction, viscous dissipation and heat generation or absorption on unsteady MHD flow past an inclined porous plate embedded in porous medium. Non dimensional form of partial differential equations of governing equations of flow has been solved by applying Crank-Nicolson implicit finite difference method. Velocity, temperature, concentration profiles are discussed through graphs for different values of parameters and skin friction coefficients, Nusselt number, Sherwood number have been discussed through tables.

2. MATHEMATICAL ANALYSIS

An unsteady MHD flow of viscous incompressible electrically conducting fluid past an inclined infinite porous plate with Thermophoresis effect, Dufour effect, Hall effect, radiation effect, viscous dissipation, chemical reaction and Heat generation or absorption are considered. x' -axis is taken along plate, y' -axis is normal to it and z' -axis is normal to $x'y'$ plane. A uniform magnetic field B_0 is considered along y' -axis and plate is electrically non-conducting. It is considered that radiation heat flux along x' -direction is negligible in comparison to y' -direction. Initially fluid and plate are at same temperature T'_∞ and concentration C'_∞ . For $t' > 0$, the plate moves with velocity u_0 , its temperature and concentration raise exponentially with time. Magnetic Reynolds number and transversely applied magnetic field are very small so induced magnetic field is negligible in comparison to applied magnetic field, Cowling(Cowling 1957).

$$\begin{aligned} J'_x &= \frac{\sigma B_0}{1+m^2}(mu' - w') \\ J'_z &= \frac{\sigma B_0}{1+m^2}(u' + mw') \end{aligned} \tag{1}$$

where u' and w' are velocities, J'_x and J'_z are electric current density along x' -axis and z' -axis respectively, m is Hall parameter. Due to infinite length in x' direction, flow variables are function of t' and y' only. Under usual Boussinesq approximation, governing equations of this problem are given by:

$$\frac{\partial v'}{\partial y'} = 0 \Rightarrow v' = -v_0(\text{constant}) \tag{2}$$

$$\begin{aligned} \frac{\partial u'}{\partial t'} + v' \frac{\partial u'}{\partial y'} &= v \frac{\partial^2 u'}{\partial y'^2} + g\gamma(T' - T'_\infty) \cos(\lambda) \\ &\quad + g\gamma^*(C' - C'_\infty) \cos(\lambda) \\ &\quad - \frac{\sigma B_0^2}{\rho(1+m^2)}(u' + mw') - \frac{vu'}{K'} \end{aligned} \tag{3}$$

$$\begin{aligned} \frac{\partial w'}{\partial t'} + v' \frac{\partial w'}{\partial y'} &= v \frac{\partial^2 w'}{\partial y'^2} \\ &\quad + \frac{\sigma B_0^2}{\rho(1+m^2)}(mu' - w') - \frac{vw'}{K'} \end{aligned} \tag{4}$$

$$\begin{aligned} \rho c_p \left(\frac{\partial T'}{\partial t'} + v' \frac{\partial T'}{\partial y'} \right) &= k \frac{\partial^2 T'}{\partial y'^2} - \frac{\partial q_r}{\partial y'} \\ &\quad + \frac{\rho D_m K_T}{c_s} \frac{\partial^2 C'}{\partial y'^2} + \mu \left(\frac{\partial u'}{\partial y'} \right)^2 \\ &\quad - Q_0(T' - T'_\infty) \end{aligned} \tag{5}$$

$$\begin{aligned} \frac{\partial C'}{\partial t'} + v' \frac{\partial C'}{\partial y'} &= D \frac{\partial^2 C'}{\partial y'^2} + \frac{D_m K_T}{T_m} \frac{\partial^2 T'}{\partial y'^2} \\ &\quad - k_r(C' - C'_\infty) \end{aligned} \tag{6}$$

where γ^* is coefficient of volume expansion for mass transfer, γ is volumetric coefficient of thermal expansion, v' is velocity along y' -axis, K' is permeability of porous medium, σ is electrical conductivity, D_m is molecular diffusivity, g is acceleration due to gravity, K_T is thermal diffusion ratio, μ is viscosity, ρ is fluid density, k is thermal conductivity of fluid, C' and T' are dimensional concentration and temperature, C'_∞ and T'_∞ are concentration and temperature of free stream, k_r is chemical reaction parameter; the term $Q_0(T' - T'_\infty)$ is considered to be amount of heat generated or absorbed per unit volume, Q_0 is constant, for heat source $Q_0 > 0$ and for heat sink $Q_0 < 0$; c_p is specific heat at constant pressure, q_r is radiative heat along y' -axis, v is kinematic viscosity and T_m is mean fluid temperature.

Boundary and initial conditional for this model are given as:

$$\begin{aligned} t' \leq 0 \quad u' &= 0 \quad w' = 0 \\ T' &= T'_\infty \quad C' = C'_\infty \quad \forall y' \\ t' > 0 \quad u' &= u_0 \quad v' = -v_0 \quad w' = 0 \\ T' &= T'_\infty + (T'_w - T'_\infty)e^{Bt'}, \\ C' &= C'_\infty + (C'_w - C'_\infty)e^{Bt'} \quad \text{at } y' = 0 \\ u' &= 0 \quad w' = 0 \quad T' \rightarrow T'_\infty \\ C' &\rightarrow C'_\infty \quad y' \rightarrow \infty \end{aligned} \tag{7}$$

where T'_w and C'_w are concentration and temperature respectively of plate and $B = \frac{v_0^2}{\nu}$.

The radiative heat flux term by using the Roseland approximation is given by

$$q_r = -\frac{4\sigma}{3k_m} \frac{\partial T'^4}{\partial y'} \tag{8}$$

$$\begin{aligned} & \frac{u_{i,j+1} - u_{i,j}}{\Delta t} - \frac{u_{i+1,j} - u_{i,j}}{\Delta y} = \\ & \left(\frac{u_{i-1,j} - 2u_{i,j} + u_{i-1,j} - 2u_{i,j+1} + u_{i+1,j+1}}{2(\Delta y)^2} \right) \\ & + Gr \cos(\lambda) \left(\frac{\theta_{i,j+1} - \theta_{i,j}}{2} \right) \\ & + Gm \cos(\lambda) \left(\frac{C_{i,j+1} - C_{i,j}}{2} \right) \\ & - \left(\frac{M}{1+m^2} + \frac{1}{K} \right) \left(\frac{u_{i,j+1} + u_{i,j}}{2} \right) \\ & - \left(\frac{mM}{1+m^2} \right) \left(\frac{w_{i,j+1} + w_{i,j}}{2} \right) \end{aligned} \tag{18}$$

$$\begin{aligned} & \frac{w_{i,j+1} - w_{i,j}}{\Delta t} - \frac{w_{i+1,j} - w_{i,j}}{\Delta y} = \\ & \left(\frac{w_{i-1,j} - 2w_{i,j} + w_{i-1,j} - 2w_{i,j+1} + w_{i+1,j+1}}{2(\Delta y)^2} \right) \\ & - \left(\frac{M}{1+m^2} + \frac{1}{K} \right) \left(\frac{uw_{i,j+1} + w_{i,j}}{2} \right) \\ & + \left(\frac{mM}{1+m^2} \right) \left(\frac{u_{i,j+1} + u_{i,j}}{2} \right) \end{aligned} \tag{19}$$

$$\begin{aligned} & \frac{\theta_{i,j+1} - \theta_{i,j}}{\Delta t} - \frac{\theta_{i+1,j} - \theta_{i,j}}{\Delta y} = \\ & \frac{1}{Pr} \left(1 + \frac{4R}{3} \right) \\ & \left(\frac{\theta_{i-1,j} - 2\theta_{i,j} + \theta_{i-1,j} - 2\theta_{i,j+1} + \theta_{i+1,j+1}}{2(\Delta y)^2} \right) + \\ Du & \left(\frac{C_{i-1,j} - 2u_{i,j} + C_{i-1,j} - 2C_{i,j+1} + C_{i+1,j+1}}{2(\Delta y)^2} \right) \\ & + Ec \left(\frac{u_{i+1,j} - u_{i,j}}{\Delta y} \right)^2 - Q \left(\frac{\theta_{i,j+1} + \theta_{i,j}}{2} \right) \end{aligned} \tag{20}$$

$$\begin{aligned} & \frac{C_{i,j+1} - C_{i,j}}{\Delta t} - \frac{C_{i+1,j} - C_{i,j}}{\Delta y} = \\ & \frac{1}{Sc} \left(\frac{C_{i-1,j} - 2u_{i,j} + C_{i-1,j} - 2C_{i,j+1} + C_{i+1,j+1}}{2(\Delta y)^2} \right) \\ & + Sr \left(\frac{\theta_{i-1,j} - 2\theta_{i,j} + \theta_{i-1,j} - 2\theta_{i,j+1} + \theta_{i+1,j+1}}{2(\Delta y)^2} \right) \\ & - Kr \left(\frac{C_{i,j+1} + C_{i,j}}{2} \right) \end{aligned} \tag{21}$$

initial and boundary conditions are also expressed as:

$$\begin{aligned} u_{i,0} = 0 \quad w_{i,0} = 0 \quad \theta_{i,0} = 0 \quad C_{i,0} = 0 \quad \forall i \\ u_{0,j} = 1 \quad w_{0,j} = 0 \quad \theta_{0,j} = e^{j\Delta t} \quad C_{0,j} = e^{j\Delta t} \\ u_{L,j} = 0 \quad w_{L,j} = 0 \quad \theta_{L,j} \rightarrow 0 \quad C_{L,j} \rightarrow 0 \end{aligned} \tag{22}$$

where index i refers to y and j refers to time t , $\Delta t = t_{j+1} - t_j$ and $\Delta y = y_{i+1} - y_i$. Knowing the values of u , θ and C at time t , we can compute the values at time $t + \Delta t$ as follows: we substitute $i = 1, 2, \dots, N - 1$, where N correspond to ∞ , equations 18 to 21 give tridiagonal system of equations with initial and boundary conditions in equation 22, are solved using Thomos algorithm as discussed in Carnahan et al.(Brice Carnahan and Wilkes 1969), we find values of θ and C for all values of y at $t + \Delta t$. Equation 18 and 19 are solved by same to substitute these values of θ and C , we get solution for u and w till desired time t .

The implicit Crank-Nicolson finite difference method is a second order method ($o(\Delta t^2)$) in time and has no restriction on space and time steps, that is, the method is unconditionally stable. The computation is executed for $\Delta y = 0.1$, $\Delta t = 0.001$ and procedure is repeated till $y = 4$.

4. RESULT AND DISCUSSION

In order to analysis, we would like to see numerical results for velocity profiles u , w along x -axis and z -axis, temperature profile θ and concentration profile C with help of graphs by assigning numerical values of thermal Grashof number Gr , solutal Grashof number Gm , Schmidt number Sc , Prandtl number Pr , Thermophoresis number Sr , Dufour number Du , magnetic parameter M , Hall parameter m , permeability of porous medium K , radiation parameter R , Eckert number Ec , chemical reaction parameter Kr , heat absorption or generation constant Q , inclination angle λ . And coefficients of skin friction τ_1 and τ_2 along x -axis and z -axis, Nusselt number and Sherwood number are discussed through tables.

Velocity profiles u and w in figure(1), temperature profile θ in figure(3) and concentration profile C in figure(2) increase when Sr increases. On increasing Schmidt number Sc , it is analyzed that concentration profile C in figure(20) decreases. Figures (4), (5), (6) depict when Prandtl number Pr increases, velocity profiles u and w first increase after then at some distance from wall it decrease, temperature profile θ decreases and concentration profile C first increases after then at some distance from wall it decreases. Figures (7), (8) and (9) depict that on increasing heat absorption or generation coefficient Q , velocity profiles u and w first increase after then decrease, temperature profile θ decreases

and concentration profile C first increases after then decreases. It is analyzed from figures(10) and (11) when Dufour number Du increases then temperature profile θ increases and concentration profile C first decreases after then increases. Velocity profile u decreases while velocity profile w increases in figure(12) when magnetic parameter M increases.

It is studied that velocity profiles u and w first decrease after then increase in figure(13), temperature profile increases in figure(14) and concentration profile C increases in figure(15) as radiation parameter R increases. It is clear that concentration profile C decreases in figure(21) as chemical reaction parameter Kr increases. Figures (16) and (17) depict that temperature profile θ increases and concentration profile C first decreases after then increases when Eckert number Ec increases. It is shown that on increasing inclination angle λ , Hall parameter m , velocity profiles u and w increase in figures (18), (19) respectively. It is analyzed from figures (22), (23), (24) that on increasing time t , velocity profiles u and w , temperature profile θ and concentration profile C increase.

It is analyzed from table(1) that Du , Ec , Kr , λ , R and Sc increase then skin friction coefficients τ_1 and τ_2 decrease while Gm , Gr , m , Pr , Q , Sr and t increase then skin friction coefficients τ_1 and τ_2 increase and on increasing M , τ_1 decreases while τ_2 increases.

On the other hand it is analyzed from table(2) when Du , Ec , Kr , λ , M and R increase then Nusselt number Nu decreases and Sherwood number Sh increases and on increasing Gm , Gr , Pr , Q and t , Nusselt number Nu increases and Sherwood number Sh decreases while on increasing m , Sc and Sr Nusselt number Nu and Sherwood number Sh decreases.

5. CONCLUSION

In this work we have analyzed Thermophoresis-Dufour and radiation effects on unsteady MHD flow past an inclined porous plate embedded in porous medium in presence of Hall effect, chemical reaction effect, heat generation and absorption and viscous dissipation. From present numerical study, the following conclusions have been drawn:

1. On increasing Dufour number Du , radiation parameter R , Eckert number Ec concentration profile first decreases after then it increases.
2. Concentration profile first increases after then it decreases when prandtl number Pr , heat absorption coefficient Q increase.
3. On increasing prandtl number Pr , heat absorption coefficient Q , temperature profile decreases.
4. On increasing magnetic parameter M , veloc-

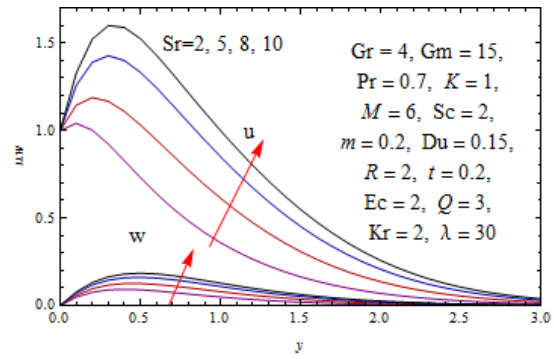


Fig. 1. Velocity Profile for Different Values of Sr

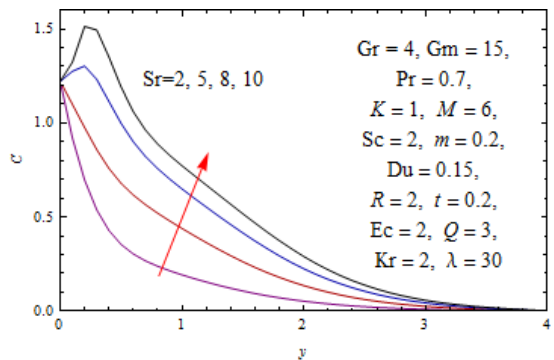


Fig. 2. Concentration Profile for Different Values of Sr

ity profile u decreases and velocity profile w increases while on

5. Velocity profiles, Temperature profile and concentration profile increase when Soret number Sr increases.
6. It has been seen that on increasing Hall parameter m , skin-friction coefficients τ_1 , τ_2 and Nusselt number Nu increase while Sherwood number Sh decreases.

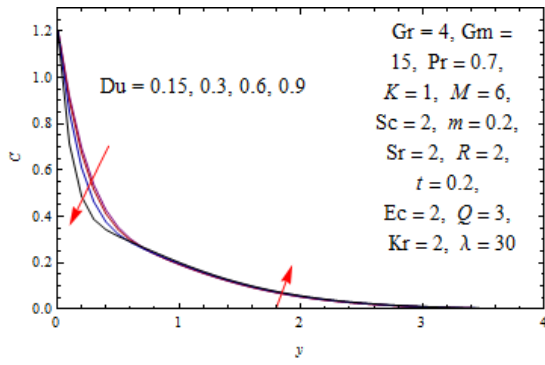


Fig. 11. Concentration Profile for Different Values of Du

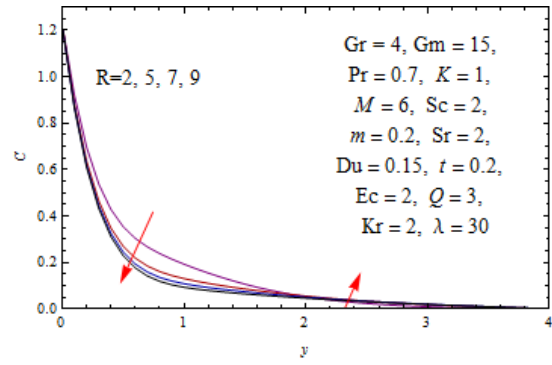


Fig. 15. Concentration Profile for Different Values of R

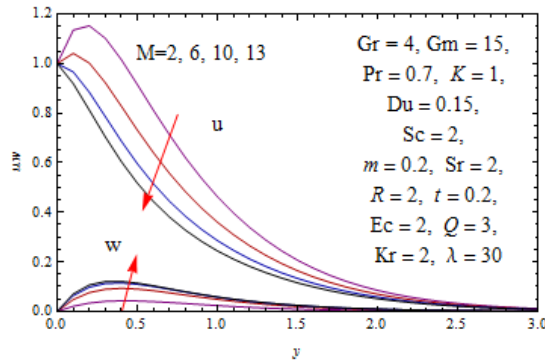


Fig. 12. Velocity Profile for Different Values of M

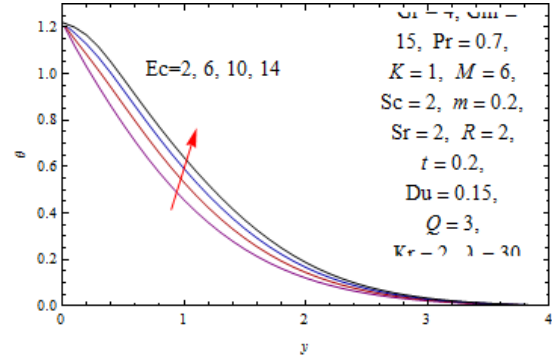


Fig. 16. Temperature Profile for Different Values of Ec

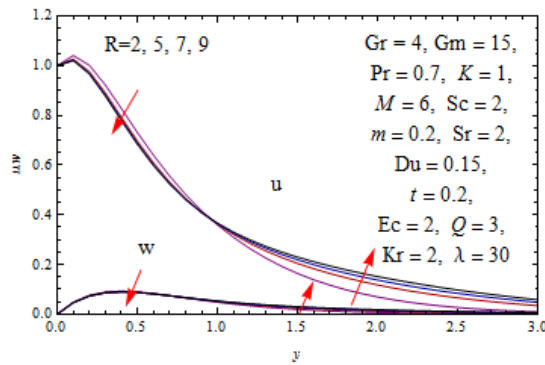


Fig. 13. Velocity Profile for Different Values of R

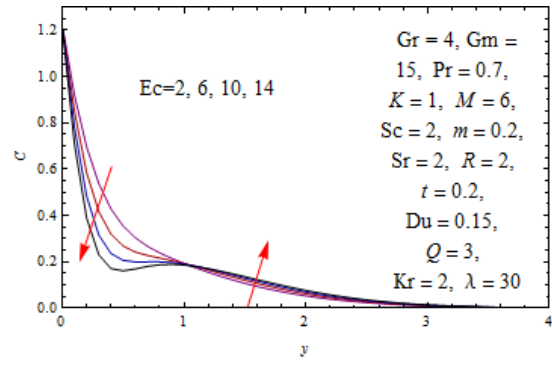


Fig. 17. Concentration Profile for Different Values of Ec

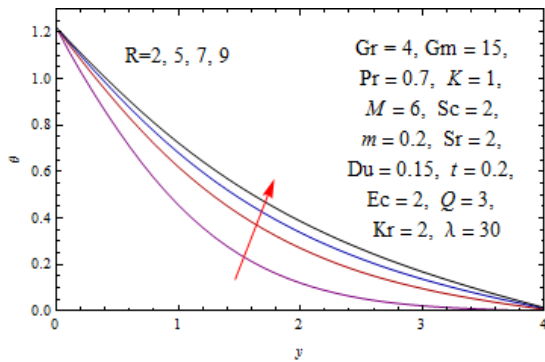


Fig. 14. Temperature Profile for Different Values of R

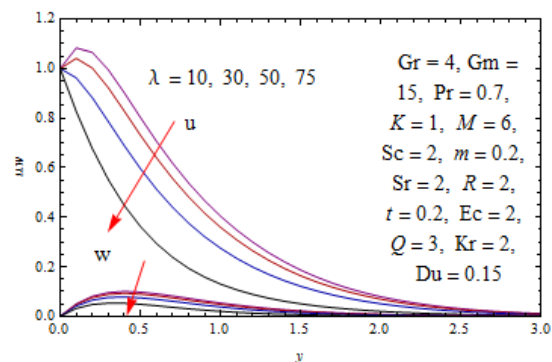


Fig. 18. Velocity Profile for Different Values of λ

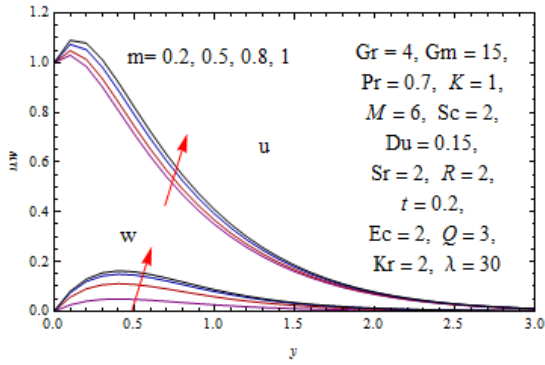


Fig. 19. Velocity Profile for Different Values of m

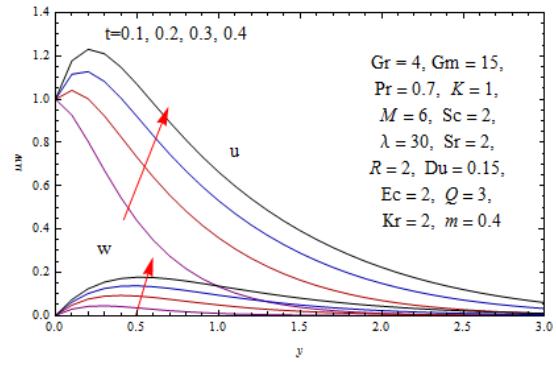


Fig. 22. Velocity Profile for Different Values of t

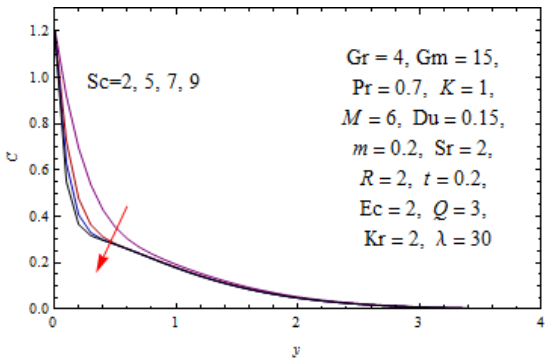


Fig. 20. Concentration Profile for Different Values of Sc

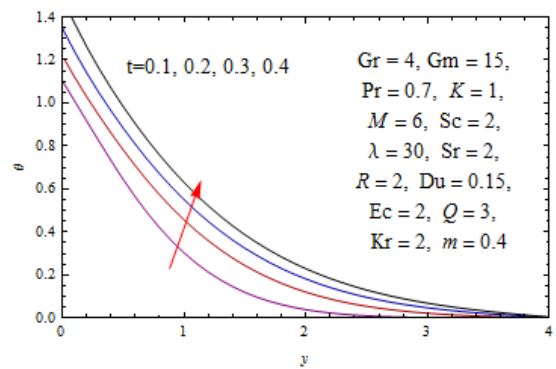


Fig. 23. Temperature Profile for Different Values of t

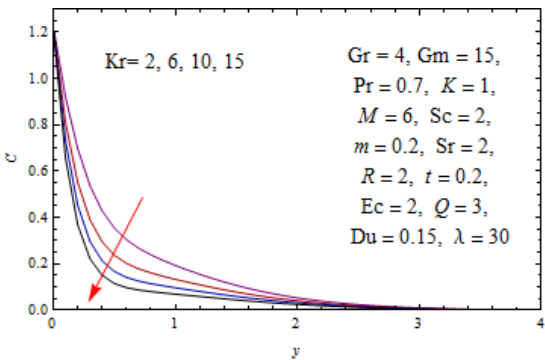


Fig. 21. Concentration Profile for Different Values of Kr

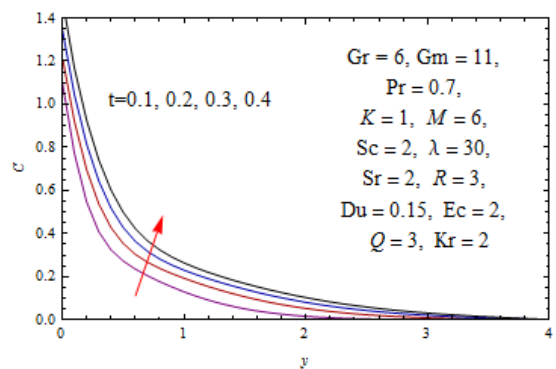


Fig. 24. Concentration Profile for Different Values of t

